

WF6-CVD tungsten film as an emitter for a thermionic energy converter I. Production, texture and morphology of WF6-CVD tungsten films

Citation for published version (APA):

Gubbels, G. H. M., Wolff, L. R., & Metselaar, R. (1989). WF6-CVD tungsten film as an emitter for a thermionic energy converter I. Production, texture and morphology of WF6-CVD tungsten films. *Applied Surface Science*, 40(3), 193-199. [https://doi.org/10.1016/0169-4332\(89\)90002-0](https://doi.org/10.1016/0169-4332(89)90002-0)

DOI:

[10.1016/0169-4332\(89\)90002-0](https://doi.org/10.1016/0169-4332(89)90002-0)

Document status and date:

Published: 01/01/1989

Document Version:

Publisher's PDF, also known as Version of Record (includes final page, issue and volume numbers)

Please check the document version of this publication:

- A submitted manuscript is the version of the article upon submission and before peer-review. There can be important differences between the submitted version and the official published version of record. People interested in the research are advised to contact the author for the final version of the publication, or visit the DOI to the publisher's website.
- The final author version and the galley proof are versions of the publication after peer review.
- The final published version features the final layout of the paper including the volume, issue and page numbers.

[Link to publication](#)

General rights

Copyright and moral rights for the publications made accessible in the public portal are retained by the authors and/or other copyright owners and it is a condition of accessing publications that users recognise and abide by the legal requirements associated with these rights.

- Users may download and print one copy of any publication from the public portal for the purpose of private study or research.
- You may not further distribute the material or use it for any profit-making activity or commercial gain
- You may freely distribute the URL identifying the publication in the public portal.

If the publication is distributed under the terms of Article 25fa of the Dutch Copyright Act, indicated by the "Taverne" license above, please follow below link for the End User Agreement:

www.tue.nl/taverne

Take down policy

If you believe that this document breaches copyright please contact us at:

openaccess@tue.nl

providing details and we will investigate your claim.

WF₆-CVD TUNGSTEN FILM AS AN EMITTER FOR A THERMIONIC ENERGY CONVERTER I. Production, texture and morphology of WF₆-CVD tungsten films

G.H.M. GUBBELS, L.R. WOLFF and R. METSELAAR

Laboratory for Physical Chemistry, Eindhoven University of Technology, P.O. Box 513, 5600 MB Eindhoven, The Netherlands

Received 7 March 1989; accepted for publication 8 August 1989

The as-deposited WF₆-CVD tungsten film consists of columnar grains about 3 μm in diameter and about 30 μm in length. The film has a <100> fiber texture with a clear tendency to the formation of a pseudo-mono-crystal. The overwhelming part of the grains have their <100> axes within 27° of the surface normal. The as-deposited film surface consists of {111} crystal planes. Two hours annealing at 2273 K resulted in grain growth leading to a grain diameter of more than 70 μm. Inspection of etch pits revealed that 62% of the surface area consists of grains which have their <100> axis within 16° of the surface normal.

1. Introduction

A thermionic energy converter (TEC) is a device which directly converts heat into electricity. It consists of two electrodes one of which (the emitter) is heated to a temperature at which it will thermally emit electrons. The other electrode (the collector) is kept at a lower temperature and collects the electrons, see fig. 1. Part of the heat removed from the emitter by evaporating electrons is rejected to the collector by condensing elec-

trons. The remaining part is converted into electric power in the load as the electrons return to the emitter potential. Thermionic converters operating in vacuum will not produce any substantial current density unless the electrode spacing is less than 5 μm. This is due to the space-charge effect.

The space-charge problem can be overcome by introducing a rarefied vapour in the interelectrode space. The vapour generally used in TEC's is cesium, as it has the lowest ionization potential of all the elements (3.89 eV). The cesium vapour will partially ionize at the hot emitter surface, forming a cesium plasma. The positive charge of the cesium ions will neutralize the negative charge of the electron cloud causing the space-charge effect. Thus the interelectrode gap can now be increased to 0.5 mm while maintaining high current densities. Furthermore, cesium will bring down both emitter and collector workfunctions (φ_e respectively φ_c). The potential diagram of a TEC is shown in fig. 2. In order to get the optimum output voltage V₀, the barrier index

$$V_b = \phi_c + V_d, \tag{1}$$

should be minimal. Consequently, the collector workfunction, φ_c, and the plasma drop V_d should preferably be as low as possible.

The plasma drop is almost linearly proportional to the cesium vapour pressure. So, in order

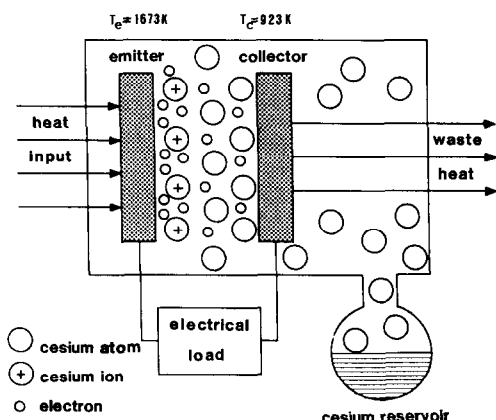


Fig. 1. Schematic drawing of a cesium vapour thermionic converter. It is a low voltage (0.5 V), high current density (10 A/cm²), direct current power source.

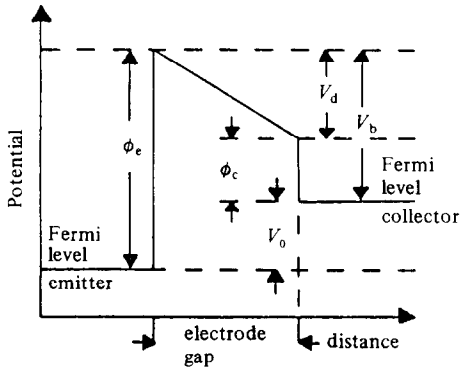


Fig. 2. Potential distribution in a thermionic energy converter.

to reduce V_d we would like to reduce this pressure. This, however, would result in a severe current density loss due to the increase of the emitter workfunction, ϕ_e [1,2]. Efforts to develop an emitter material with an optimal workfunction are the subject of this paper.

It is the aim of our research group to develop a combustion heated thermionic energy converter for industrial application [3]. A cut-away view of our design of a TEC is shown in fig. 3. In order to facilitate the commercial application of TEC's,

higher efficiencies and lower material and manufacturing costs are desired. As an emitter for a TEC we propose to use plasma sprayed tungsten [4]. This will result in relatively low material and manufacturing costs. The workfunction of a tungsten emitter surface (ϕ_e) depends on the nature of the lattice planes constituting the surface. Crystal faces with the highest workfunction in vacuum will give the best efficiency in a cesiated TEC [1,2]. Therefore, the {110} crystal faces of tungsten with a high workfunction in vacuum ($\phi = 5.22$ eV) [1,2] are preferred at the surface. The grains in plasma sprayed tungsten are randomly orientated, i.e. the plasma sprayed tungsten has no texture. Consequently, the lattice planes that constitute the polished macroscopic surface of the emitter have a random orientation relative to the main axes of the tungsten crystal lattices.

In the present work we describe an investigation into the possibility to improve the efficiency of a randomly orientated tungsten emitter by depositing a textured tungsten film on the emitter surface. In order to get an idea of the sharpness of the texture that is required in emitter material, the effective workfunction (ϕ_{eff}) of a surface com-

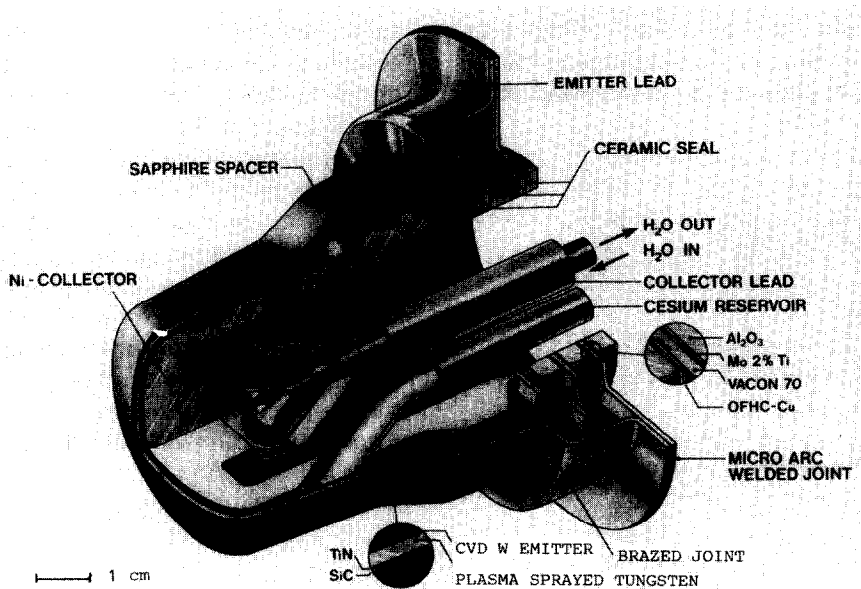


Fig. 3. Eindhoven University of Technology design of a combustion heated, water cooled, thermionic energy converter.

posed of {110} crystal planes with a fraction F of {116} crystal planes is deduced. These two planes are chosen because they have the highest and the lowest workfunction (5.22 and 4.3 eV respectively). The current density (in A/cm²) from a pure uniform surface is:

$$I = 120T_e^2 \exp(-\phi/kT_e), \quad (2)$$

where T_e is the emitter temperature in K, ϕ the workfunction in eV, and k the Boltzmann constant.

The current from a pure nonuniform surface is governed by an effective workfunction ϕ_{eff} . The current from the nonuniform surface is the sum of the current from the (110) area and the (116) area. For the effective workfunction of the nonuniform surface we get the formula:

$$\exp(-\phi_{\text{eff}}/kT_e) = F \exp(-\phi_{(116)}/kT_e) + (1 - F) \exp(-\phi_{(110)}/kT_e), \quad (3)$$

where F is the fraction of the surface area composed of (116) crystal plans. In fig. 4 the effective workfunction as a function of the (116) area fraction (F) is shown. We can conclude that the amount of alien crystal planes has to be as small as possible in order to profit from a <110> texture. A reduction of the fraction F from 0.1 to 0.01 in the hypothetical "nonuniform (1 - F)(110) + F (116)" emitter surface will decrease the current

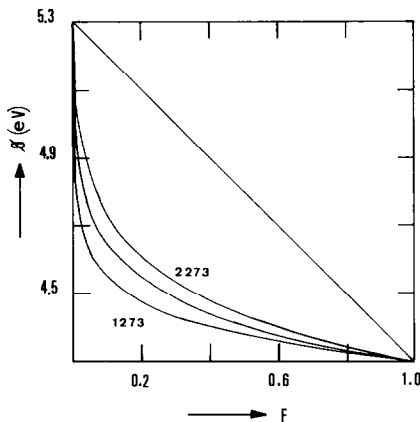


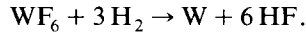
Fig. 4. Calculated effective workfunction of a (110) surface area having a fraction F of (116) planes. The emitter temperature T_e is indicated (1273, 1773 and 2273 K).

density by circa a factor 14.

It is known that various textures can be produced by the technique of chemical vapour deposition (CVD) [5,6]. In the first part of our paper we describe the texture and morphology of as-deposited and annealed WF_6 -CVD tungsten films. In part II of this paper [7] we describe the electron and Cs^+ -ion emission properties of these films.

2. CVD of tungsten films from WF_6

Tungsten films were deposited by CVD in a vertical stainless steel hot wall reactor. To achieve this, WF_6 was reduced according to the reaction:



Deposition was carried out at 1173 K using 1 mm thick tungsten substrates. The substrates were spark machined from a sintered tungsten rod. The diameter of the plane substrate was 13 mm. The substrates had no texture. The total pressure during the CVD process was 4 mbar at a H_2/WF_6 ratio of 10. The WF_6 used was of electronic grade purity. These conditions resulted in a surface-reaction-limited deposition rate of 30 $\mu\text{m/h}$. We found an activation energy of 43 ± 2 kJ/mol for this CVD process [8]. The Vickers hardness of the as-deposited film was found to be $HV = 548$ kgf/mm². The load used in the hardness measurement was 0.1 kgf. Festa and Danko [9] found a relation between the fluorine content and the hardness of the CVD film. From the measured hardness we estimate the fluorine content of the tungsten film to be 20 ppm. A large fluorine content slows down the grain growth in the film [9]. Probably the fluorine content is of importance for the electron emission properties as well.

After the deposition, one of the W-disks was incorporated, as an emitter, into a research diode. The experiments carried out in this research diode are described in part II of this paper.

3. Morphology and texture of the WF_6 -CVD tungsten film

Scanning electron microscope (SEM) photographs of the surface and of a cross section of the

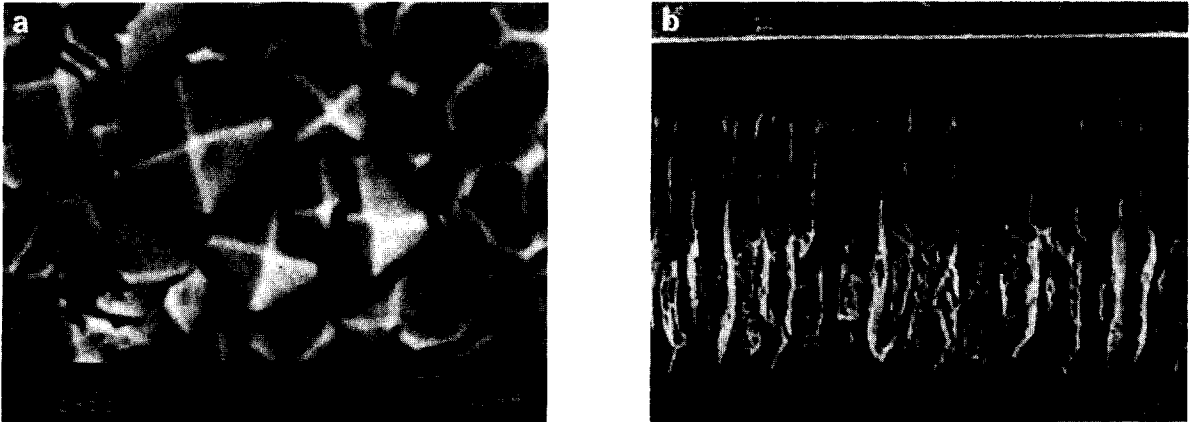


Fig. 5. SEM pictures of the as-deposited WF_6 -CVD tungsten film: (a) top view – four-sided pyramids bounded by $\{111\}$ planes; (b) etched (Murakami etching) cross section, at the upper side the tungsten substrate is visible.

as-deposited film are shown in fig. 5. The $30\ \mu\text{m}$ thick film consists of columns about $3\ \mu\text{m}$ in diameter. The top of a column is a four-sided pyramide. The interplanar angle at the top is smaller than 90° . From this morphology the surface planes are identified to be $\{111\}$ planes. The texture of the film has been investigated using a cylindrical texture camera [10]. In fig. 6 the X-ray diffraction patterns obtained are presented. As a result of the cylindrical geometry of the camera the diffraction cones of constant 2θ intersect the recording film in straight lines. A bell shape of the composition of reflections is visible. Going from the top to the bottom in a vertical direction the 2θ Bragg angle increases. At each

reflection the Miller indices of the corresponding lattice planes are indicated. In the horizontal directions, the distribution of the angles which the specified lattice planes make with the normal to the sample (i.e. the tilt angle ρ), is represented. This angle is zero on a central vertical line in the figure. If no texture is present in the sample, the reflections should continuously extend over the whole horizontal range. A Siemens X-ray texture goniometer after Lücke, with an automatic pole figure plotter has been used as well. Resulting pole figures are shown in fig. 7. During the measurement, the angle between the primary X-ray beam and the detector is kept at a fixed value of 51.30° . This angle corresponds to the 2θ Bragg angle of

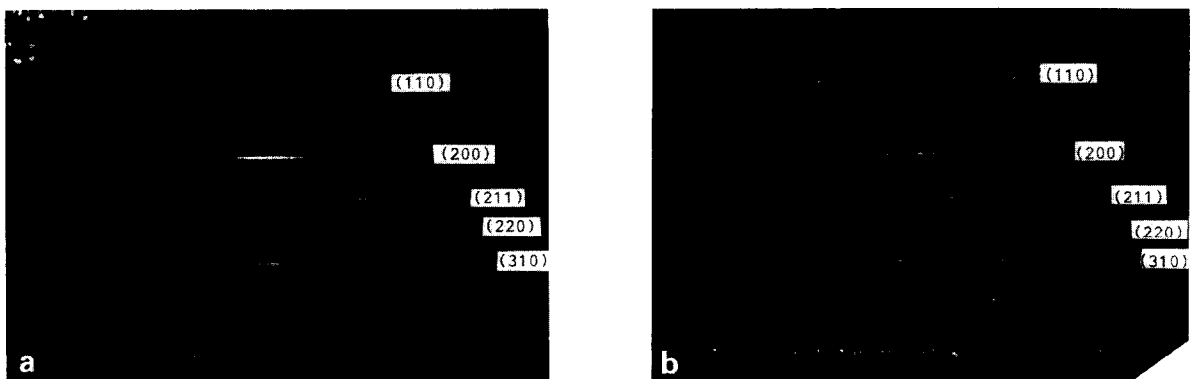


Fig. 6. X-ray pattern of the tungsten film obtained using a cylindrical camera. $Cu\ K\alpha$ radiation was used. The angle of incidence of the primary beam is 30° . The sample is not rotated. (a) The as-deposited tungsten film. (b) The annealed film (2 h at 2273 K).

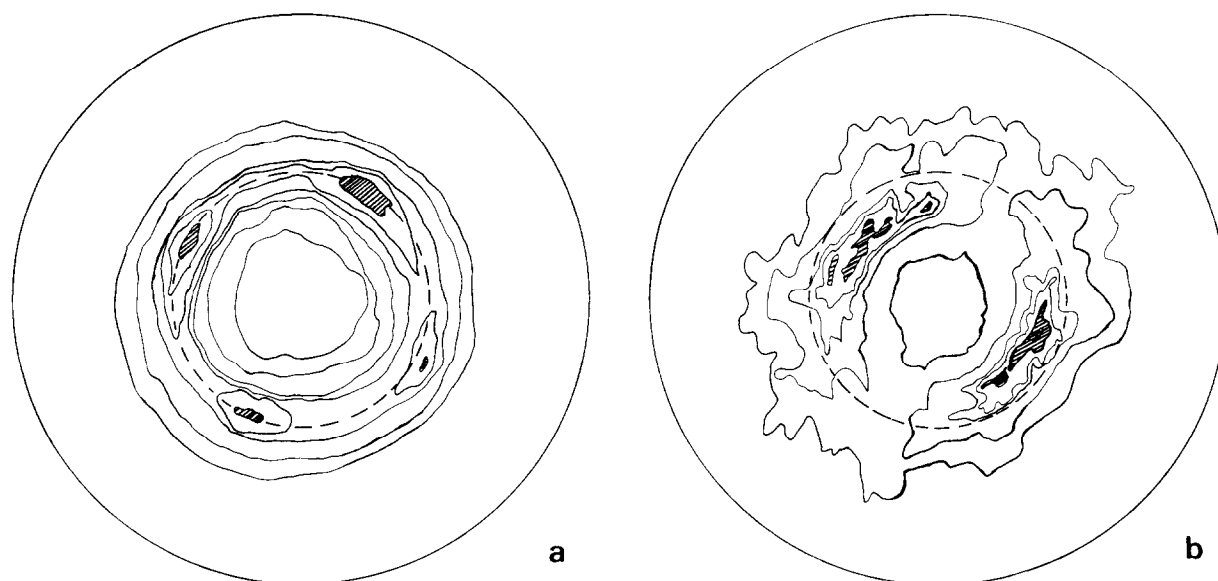


Fig. 7. $\{110\}$ pole figures of the tungsten films obtained with a Siemens texture goniometer. Fe $K\alpha$ radiation was used. (— — —) angle of 45° ; (/////) region of maximal intensity; (——) lines of equal intensity, every next line corresponds to a lower intensity (10% of the maximal intensity). (a) As deposited WF_6 -CVD tungsten: four $\{110\}$ poles can clearly be identified, indicating that apart from a fiber texture there is an inclination to form a pseudo-mono-crystal. (b) The annealed film (2 h at 2273 K).

the $\{110\}$ lattice planes. The reflected X-ray intensity is recorded while the sample is tilted and rotated. Going from the centre to the rim of the pole figure, the sample is tilted from 0° to 90° . Going around in a circular movement in the figure corresponds with an equivalent rotation of the sample around an axis perpendicular to the sample surface. At the centre of this $\{110\}$ pole figure the intensity is low because in this sample there are almost no $\{110\}$ planes that are parallel to the sample surface. The lines in the pole figure are lines of equal intensity (as on a contour map). For further details we refer to the literature [11].

Fig. 6a shows that the Bragg reflections of the $\{200\}$ lattice form are concentrated in a small region around the centre of the diffraction line. This means that a $\langle 100 \rangle$ texture is present. From the width of the 200 reflection we have calculated that grains with a $[100]$ crystal axis deviating up to 27° from the normal to the substrate, are present [8,10]. Thus the $\langle 100 \rangle$ axis of the tungsten crystal lattice of a column is tilted relative to the substrate surface. The maximal tilt angle of the $\langle 100 \rangle$ crystal axis of a column (ρ_m) is: $\rho_m = 27^\circ$. Fig. 7a

confirms that a $\langle 100 \rangle$ “fiber” texture is present because in the $\{110\}$ pole figure, maximum intensity is found at a tilt angle of 45° . Four $\{110\}$ poles can be observed in the $\{110\}$ pole figure. This indicates that the film is a pseudo-mono-crystal.

When used as an emitter in a TEC, the tungsten film will be heated for a long time at about 1673 K. In order to investigate the annealing process of the tungsten film, we have heated a mechanically polished film for 2 h at 2273 K in vacuum. The grain size increases to $70 \mu\text{m}$. The annealed film has been investigated by X-ray diffraction. The X-ray pattern, obtained with a cylindrical camera, while the sample does not rotate, is shown in fig. 6b. The spotted appearance of the reflections is a consequence of the coarse crystallinity of the annealed film. The concentration of the 200 Bragg reflections in a small region around the centre of the diffraction line indicates the presence of a $\langle 100 \rangle$ texture. This is confirmed by the splitting up of the 110 Bragg reflections in two regions, see fig. 6. As expected in a $\langle 100 \rangle$ texture the angle between these two regions is 90° .

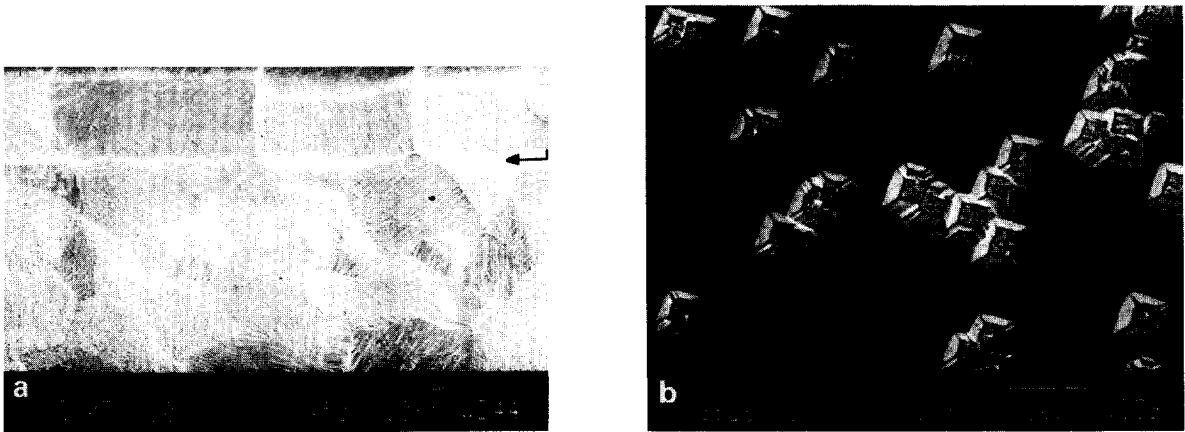


Fig. 8. Cross section and top view of a tungsten CVD coated sample subjected to the following treatments: (1) mechanical polishing, (2) heat treatment: 2 h at 2273 K in a vacuum, (3) electrolytical etching. (a) Cross section showing the results of thermally activated grain growth in the film. (b) Etch pits on the surface indicating a (106) crystal plane.

The X-ray pattern of a sample which was rotated during the measurement had no spotted appearance. The width of the 200 reflection in this pattern was changed, compared to the pattern of the as-deposited film. A maximal tilt angle $\rho_m = 36^\circ$ was found for the annealed film. The $\{110\}$ pole figure obtained with the Siemens texture goniometer does not explicitly show a $\langle 100 \rangle$ texture, cf. figs. 7a and 7b. This may be caused by the coarse grains in the annealed tungsten film, the

rather weak texture and the resulting strong influence of defocussing.

The surface of the annealed tungsten film was electrolytically etched for 50 s in a 3% NaOH solution at 2 V. SEM pictures of a cross section and of an electrolytically etched surface of the annealed film are shown in fig. 8. From the geometry of the etch pits found on the various grains in the surface, the crystallographic nature of the surface can be determined [12]. The abundance of the various types of etch pits is plotted in a standard stereographic projection (see fig. 9). This figure gives an indication of abundance of the various crystal faces at the surface. From fig. 9 it is deduced that 62% of the polished surface area consists of crystals which have their $\langle 100 \rangle$ axes within 16° of the substrate normal. It is remarkable that the grains prefer an orientation between $\langle 100 \rangle$ and $\langle 112 \rangle$.

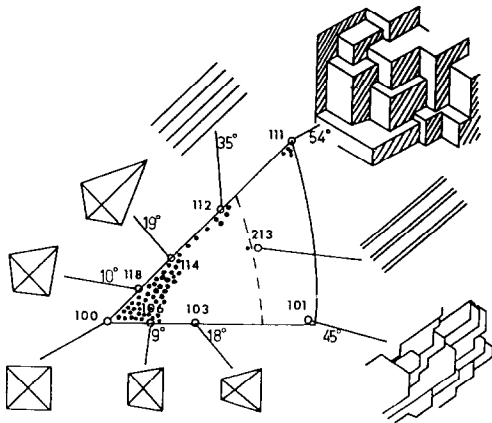


Fig. 9. In a standard stereographic projection, the various crystal planes with their characteristic etch pits are shown. The abundance of the various crystal planes on the surface of the annealed film (2 h at 2273) is indicated by dots. (— — —) Maximal tilt angle (ρ_m) in the annealed film found by X-ray diffraction.

4. Discussion and conclusions

A $\langle 110 \rangle$ textured tungsten film with a $\{110\}$ surface is the most desirable as an emitter in a thermionic energy converter, because such a film will have the best electron emission properties in a cesium filled TEC. We have deposited the tungsten films on texture-free tungsten substrates. By X-ray diffraction, we found a $\langle 100 \rangle$ fiber texture

in the as-deposited tungsten films. The surface is composed of {111} lattice planes. By X-ray diffraction in a cylindrical camera, the annealed film also showed a $\langle 100 \rangle$ texture. The maximal tilt angle was found to increase from 27° in the as-deposited film to 36° in the annealed film. The maximal tilt angle present in the annealed film, is indicated as a boundary line in the standard stereographic projection reproduced in fig. 9. Detailed inspection of the surface of the annealed film after electrolytical etching showed that 62% of the surface area was within 16° of the (100) crystal plane. In fig. 8a it is seen that a grain in the film grows together with a grain in the substrate. As the film is thin ($30 \mu\text{m}$), the growth of the grains in the film during annealing at 2273 K was probably influenced by the randomly orientated grains in the substrate.

The plasma sprayed tungsten used in a TEC as a substrate for the CVD tungsten film and the substrate used in the annealing experiment at 2273 K, are free from texture. In a TEC the emitter is heated up to a merely 1673 K. At this lower temperature the grain growth rate is lower [13]. However, the heating is supposed to be performed for a long time (40 000 h). From the experiments described in part II it is clear that grain growth (up to $100 \mu\text{m}$) occurs during the life (2000 h) of the CVD film as an emitter (1673 K). Thus the grain size is of the same order of magnitude, both after annealing at 2273 K and after the experiments in the TEC. We expect the texture to be the same in both cases as well. A WF_6 -CVD tungsten emitter surface which is polished parallel to the substrate surface will consist predominantly of {100} crystal planes and its vicinal planes. In part II the electron emission properties of the $\langle 100 \rangle$ tungsten film are described.

Acknowledgements

The authors are grateful to J. Smits of Philips CFT for the production of the CVD tungsten films. Thanks are also due to H. van Beek who has carried out the X-ray diffraction measurements.

References

- [1] G.N. Hatsopoulos and E.P. Gyftopoulos, *Thermionic Energy Conversion*, Vols. I and II (MIT, Cambridge, MA, 1979).
- [2] F.G. Baktsh, G.A. Dyuzhev, A.M. Martsinnovskiy, B.Ya. Moyzhes, G.Ye. Pikus, E.B. Sonin and V.G. Yur'yev, *Thermionic Converters and Low Temperature Plasma*, English ed., Ed. L.K. Hansen, DOE tr11 (Technical Information Center, Springfield, VA, 1978).
- [3] G.H.M. Gubbels, R. Metselaar, E. Penders and L.R. Wolff, in: *Proc. 21th Intersociety Energy Conversion Engineering Conf.*, Eds. J.C. Mitchell and H. Arastoopour (American Chemical Society, Washington, DC, 1986) p. 1343.
- [4] L.R. Wolff, J.M. Hermans, J. Adriaansen and G.H.M. Gubbels, in: *High Tech. Ceramics*, Ed. P. Vincenzini (Elsevier, Amsterdam, 1987) p. 2397.
- [5] Y. Pauleau, *Bull. Soc. Chim. France* 4 (1985) 583.
- [6] *Gmelin Handbuch der Anorganischen Chemie, Wolfram, Ergänzungsband a1*, Ed. F. Benesovsky (Springer, Berlin, 1979).
- [7] G.H.M. Gubbels, L.R. Wolff and R. Metselaar, *Appl. Surface Sci.* 40 (1989) 201.
- [8] G.H.M. Gubbels, *Chemical Vapour Deposited Tungsten as Emitter in a Thermionic Energy Converter*, Progress Report no. 6 (ISBN 90-6819-009-1, Eindhoven University of Technology, Eindhoven, 1989).
- [9] J.V. Festa and J.C. Danko, in: *Proc. Intern. Conf. on Chemical Vapour Deposition*, Gatlinburg, TN, 1967, Ed. A.C. Schaffhauser.
- [10] C.A. Wallace and R.C.C. Rand, *J. Appl. Cryst.* 8 (1975) 255.
- [11] B.D. Cullity, *Elements of X-Ray Diffraction* (Addison-Wesley, Reading, MA, 1967).
- [12] J.R. Thomson, J.C. Danko, T.L. Gregory and R. Webster, *IEEE Trans. Electron Devices* ED-16 (1969) 707.
- [13] Y.T. Auck and J.G. Byrne, *J. Mater. Sc.* 8 (1973) 559.